water

MDPI

Article

Tritium Transport in the Transboundary Neris River During the Routine Operation of the Belarusian Nuclear Power Plant: A Monitoring and Modeling Approach

Žana Skuratovič [1,*], Jonas Mažeika [1], Rimantas Petrošius [1], Olga Jefanova [1], Vitaliy Romanenko [1], Ričardas Paškauskas [2], Boris Adamovich [3] and Ali Erturk [1,4]

[1] Laboratory of Nuclear Geophysics and Radioecology, State Scientific Research Institute Nature Research Centre, Akademijos Str. 2, 08412 Vilnius, Lithuania
[2] Laboratory of Algology and Microbial Ecology, State Scientific Research Institute Nature Research Centre, Akademijos Str. 2, 08412 Vilnius, Lithuania
[3] Research Laboratory of Aquatic Ecology, Faculty of Biology, Belarusian State University, 220030 Minsk, Belarus
[4] Department of Freshwater Resources Management, Faculty of Aquatic Sciences, Istanbul University, Istanbul 34134, Türkiye
* Correspondence: zana.skuratovic@gamtc.lt

Abstract

This study presents long-term observations of tritium (^{3}H) concentrations in the Neris River at monitoring sites located near the Belarus–Lithuania border and in the city of Vilnius. Since the commissioning of the Belarusian Nuclear Power Plant (BelNPP), ^{3}H levels in the river have consistently exceeded natural background values, with pronounced temporal variations. These fluctuations are attributed to routine ^{3}H releases from the BelNPP, with increased concentrations observed during scheduled maintenance periods. A ^{3}H transport model was developed to estimate the downstream propagation of releases and to assess the time lag between upstream discharge events and their detection at downstream locations. The model reliably simulates ^{3}H behavior in flowing water and can be adapted to future scenarios and other water-soluble radionuclides, provided that isotope-specific and hydrological data are available. These findings highlight the importance of continued monitoring and further research on the fate and transport of radioactive substances in transboundary river systems.

Keywords: tritium (^{3}H); Belarusian Nuclear Power Plant; riverine transport modeling; Neris River; advection–decay model; GoldSim

Academic Editor: Hucai Zhang

Received: 7 July 2025
Revised: 18 August 2025
Accepted: 26 August 2025
Published: 1 September 2025

Citation: Skuratovič, Ž.; Mažeika, J.; Petrošius, R.; Jefanova, O.; Romanenko, V.; Paškauskas, R.; Adamovich, B.; Erturk, A. Tritium Transport in the Transboundary Neris River During the Routine Operation of the Belarusian Nuclear Power Plant: A Monitoring and Modeling Approach. *Water* **2025**, *17*, 2580. https://doi.org/10.3390/w17172580

1. Introduction

Tritium (^{3}H) is a radioactive isotope of hydrogen, with a half-life of 4500 ± 8 days [1], occurring both naturally and from anthropogenic activities, typically in low concentrations within the hydrological cycle. In the atmosphere, ^{3}H is primarily generated in the stratosphere by the interaction of thermal neutrons with nitrogen-14 (^{14}N) and subsequently decays into helium-3 (^{3}He) through beta emission, with a maximum energy of 18 keV. Chemically, ^{3}H behaves similarly to the stable hydrogen isotopes protium (^{1}H) and deuterium (^{2}H), integrating into the water molecule as part of H_2O. This makes it an ideal tracer for studying surface and subsurface hydrological processes [2]. Due to its radioactive nature and relatively short half-life, ^{3}H concentrations decrease measurably over time, enabling its use in estimating the age and movement of water in hydrological systems.

Natural ^{3}H-specific activity in surface waters typically ranges between 0.1 and 0.9 Bq/L, depending on geographic and climatic conditions [3]. The use of ^{3}H is well established in hydrology as an isotopic tracer for determining the age of recent (<60 years) groundwater in aquifers, aiding assessment of their vulnerability [4].

^{3}H content is often expressed as the ratio of ^{3}H to protium and reported in "tritium units" (TUs), where 1 TU corresponds to one atom of ^{3}H per 10^{18} atoms of protium. In contrast, radioecology and radiation protection practices typically employ activity-based units, with the becquerel (Bq) being the most commonly used, defined as one disintegration per second. As both units are relevant for this study, their equivalence is defined as 1 TU = 0.11919 $\pm$ 0.00021 Bq/kg [5]. Excessive ^{3}H in freshwater may occur locally around nuclear facilities, such as power plants, research reactors, and reprocessing plants, or result from large-scale atmospheric releases, such as the global ^{3}H "bomb peak" of the 1960s caused by nuclear weapons testing [3,6]. Its environmental mobility and sensitivity make ^{3}H both a valuable tracer and a radiological indicator of nuclear facility discharges [6,7].

Numerous studies have documented ^{3}H concentrations in surface waters surrounding nuclear facilities, showing clear increases during reactor operation and declines after closure. For instance, long-term monitoring of the Vltava River in the Czech Republic captured changes in ^{3}H levels before and after the commissioning of the Temelín NPP [8]. ^{3}H has also been applied to groundwater studies, such as the work of Gusyev et al. [9], which successfully integrated isotopic data into transient transport models, enhancing the simulation of groundwater residence times. Additional research has investigated ^{3}H dynamics focused on air–water exchange, such as [10] modeling the transfer of ^{3}H from surface water to the atmosphere in the context of NPP releases into the Loire River (France). Similarly, Schubert et al. [11] used ^{3}H and radon to study groundwater discharge into the Elbe River under low-flow conditions. At the ecosystem level, Galeriu and Melintescu [12] developed a model to predict the formation of organically bound ^{3}H in aquatic food webs, emphasizing the importance of monitoring ^{3}H uptake by organisms. On a broader scale, a three-dimensional global model developed by Chang Zhao et al. [13] simulated ^{3}H transport and dispersion following the Fukushima Daiichi NPP accident, highlighting potential impacts on marine ecosystems and public health.

In Lithuania, isotopic studies, particularly of ^{3}H, have been conducted since the operation of the Ignalina Nuclear Power Plant (INPP), with Lake Druksiai providing the longest monitoring record. During the INPP operation, elevated ^{3}H concentrations were recorded in the lake, peaking at 201.3 $\pm$ 1.3 TU in 2003, compared to background values of approximately 9.2 $\pm$ 3.5 TU in other surface waters at that time [14]. Following the plant's shutdown and subsequent decommissioning, ^{3}H levels in Lake Druksiai declined markedly, reaching near-background values of 19–27 TU by 2016. These observations illustrate how ^{3}H concentrations in aquatic systems increase during NPP operation and gradually return toward background levels after closure, albeit with a time lag. Notably, the observed ^{3}H concentrations remain above the relatively low maximum permissible limit of 839 TU (100 Bq/L) set by Lithuanian drinking water standards [15], which is considerably more stringent than international guidelines such as those of Canada (58,730 TU, 7000 Bq/L) or the United States (6209 TU, 740 Bq/L) [14].

Within reactors, ^{3}H is generated in fuel elements, structural components, and coolant systems and can be transported throughout the plant via gaseous and liquid pathways. Its monitoring is essential for assessing radiological dynamics in aquatic environments [16,17]. The mechanisms of ^{3}H production in nuclear reactors are comprehensively described by the IAEA (1981) [18]. Since the first nuclear power plant (NPP) began operating in 1954 in Obninsk, Russia, the number of reactors has grown to over 418 worldwide, producing approximately 10% of global electricity needs. This milestone marked the beginning

of nuclear technology as a viable source of large-scale electricity generation. Since then, nuclear energy has expanded considerably, with countries such as the United States, France, China, and Russia becoming leading producers. As of 2023, 418 nuclear reactors were in operation worldwide, with a combined capacity of 377.6 GW(e) [19].

Many nuclear power plants are located near rivers for cooling and operational needs, making rivers potential pathways for ^{3}H dispersion. Examples include the Biblis NPP (Germany) on the Rhine River, Browns Ferry NPP (USA) on the Tennessee River in Alabama, Gravelines NPP (France) near the Aa River, and Kaiga NPP (India) near the Kali River in Karnataka. Rivers often serve as conduits for the release and dispersion of ^{3}H into the environment—either through routine operational discharges or accidental releases. Tritium releases from NPPs are typically within regulatory limits; however, the cumulative impact of routine discharges, particularly into transboundary rivers, warrants detailed investigation.

In the Eastern Baltic region, the commissioning of Unit I of the Belarusian Nuclear Power Plant (BelNPP) at the end of 2020 and Unit II in mid-2023 has increased interest in ^{3}H monitoring. The BelNPP is situated near the town of Ostrovets in western Belarus, within the Neris (Viliya) River catchment and approximately 20 km from the Lithuanian border. It is also located close to the Lithuanian capital, Vilnius, about 50 km downstream. The facility comprises two pressurized water reactors (PWRs) with a combined installed capacity of approximately 2.4 GW. Each reactor operates on a fuel cycle of 5–6 years, after which the spent fuel is stored on-site in cooling pools for an additional 5–10 years to allow for decay heat dissipation. Reported safety systems include four independent and redundant barriers: a core melt trap, a double containment structure, a hydrogen removal system, and passive heat removal mechanisms. Additional passive safety is provided by fuel pellets sealed in fuel rods, a multi-loop cooling circuit, and a reinforced containment structure approximately 1 meter thick. The plant is designed for an operational lifespan of 60 years [20].

A potential transboundary aquatic pathway for radionuclide transport from the Belarusian BelNPP is the Neris River, which, through the hydraulic tunnel, receives liquid discharges from the plant. Flowing northwest, the Neris River passes through Vilnius before joining the Nemunas River. It is the largest tributary of the Nemunas—the main river discharging to the Baltic Sea—and the second-longest river in Lithuania, with a total length of 498 km, including 264 km within Belarus [21]. Nevertheless, no published data have been available until now on tritium dynamics in river systems influenced by the BelNPP. Since the very beginning of the BelNPP's operation, increased ^{3}H levels exceeding natural background concentrations have been detected in the Neris River—both near the Belarusian border and further downstream in Vilnius. This prompted the consideration of a dynamic riverine transport model to interpret the spatiotemporal distribution of observed ^{3}H data. In this context, the present study has the following aims:

(1) To evaluate long-term trends in ^{3}H concentrations at two key monitoring sites—near the Belarus–Lithuania border and in Vilnius;
(2) To assess the relationship between observed ^{3}H fluctuations and operational phases of the BelNPP, including scheduled maintenance periods;
(3) To apply a hydrological transport model to simulate the movement and attenuation of ^{3}H under various discharge scenarios.

The developed model may also serve as a framework for assessing the fate of other water-soluble radionuclides in comparable riverine environments.

2. Materials and Methods

This study was conducted on the Neris River, a transboundary watercourse originating in Belarus and flowing into Lithuania. Two long-term monitoring sites were selected:

one approximately 2 km downstream of the Belarus–Lithuania border (hereafter referred to as the "border site") and another within the city of Vilnius, approximately 130 km downstream. The Neris River is the primary surface water body in the region, serving important ecological functions and providing socioeconomic benefits.

2.1. Sampling and Analytical Methods

Atmospheric precipitation for ^{3}H analysis was collected at two sampling sites in eastern Lithuania, Zarasai (55°43′46″ N, 26°10′42″ E, WGS) and Vilnius (54°46′40″ N, 25°17′36″ E, WGS), with sampling initiated in 1999 and 2017, respectively. A cylindrical stainless steel precipitation collector with a 50 cm diameter was used. As samples were analyzed monthly, the collector was also cleaned and rinsed at the time of container replacement.

Surface water samples were collected to determine the specific activity of ^{3}H in the Neris River. Regular monthly sampling was conducted at a site near the Belarusian border (54°50′20″ N, 25°44′30″ E, WGS), beginning in February 2017 and continuing to the present. In addition, to support high-resolution ^{3}H transport modeling, daily water sampling was carried out at the Vilnius site (54°44′47″ N, 25°17′35″ E, WGS) throughout 2023, yielding 365 samples. Samples were collected using a 1 L stainless steel sampler following standardized surface water monitoring protocols to ensure methodological consistency and comparability across sites. The locations of the river sampling sites are shown in Figure 1. The Zarasai atmospheric precipitation sampling site is not included in the figure.

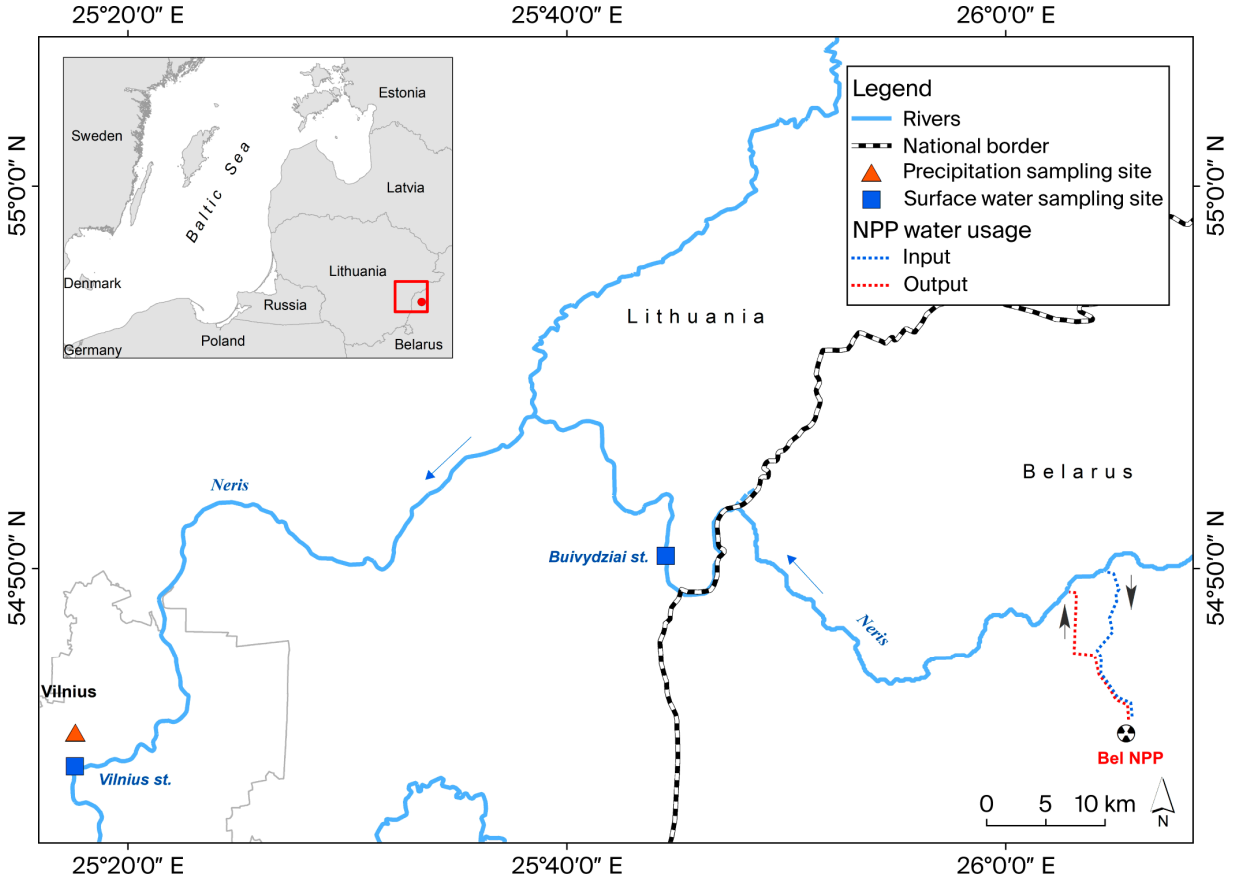

Figure 1. The locations of the sampling sites. The arrows near the nuclear plant reflect the sites of water intake for the plant and discharge to the Neris River. The map was produced using ArcGIS for illustrative purposes only.

The ^{3}H activity concentration in atmospheric precipitation and surface water was measured using liquid scintillation counting (LSC) techniques [22–24]. For routine analysis, 8 mL of the water sample was mixed with 12 mL of ULTIMA GOLD LLT scintillation cocktail and measured using LSC. All monthly atmospheric precipitation samples, as well as the monthly samples from the Neris River near the Belarusian border, were subjected to a multi-step preparation process, including pre-distillation, electrolytic enrichment, neutralization, final distillation, and mixing with the scintillation cocktail [25]. The resulting samples were then analyzed using high-precision LSC decay counting. In contrast, the daily surface water samples collected from the Neris River in Vilnius during 2023 were analyzed using direct LSC without enrichment or pre-treatment due to the large number of samples processed.

The beta spectra of all samples were measured using an ultra low-level liquid scintillation spectrometer (1220 QUANTULUS). With a background counting rate for ^{3}H below 1 CPM, a counting efficiency of approximately 25%, and an enrichment factor of ~27, the minimum detection limits for ^{3}H were estimated at 5.4 TU for direct counting and 0.2 TU following electrolytic enrichment. Quality control procedures included using reference standards and blanks in each measurement batch, along with replicate analyses for selected samples [5]. The routine performance of ^{3}H determinations in our laboratory—both by direct counting and after enrichment—was positively evaluated in the IAEA intercomparison exercises on low-level tritium in water (TRIC2004, TRIC2008, TRIC2012, TRIC20218, and TRIC2022), with satisfactory results based on z-scores (bias) and zeta tests (uncertainty) [26].

2.2. Hydrological Data

Daily river discharge data (in m^3/s) for 2018–2023 were obtained from the Lithuanian Hydrometeorological Service for three gauging stations [27–32]): two on the Neris River (at Buivydziai and Vilnius) and one on the Zeimena River, a tributary upstream of its confluence with the Neris. Discharge values corresponding to sampling dates were used both for the contextual interpretation of ^{3}H concentration data and as input parameters for the transport model. To characterize the Neris River in more detail, river cross-section data were also required. Some cross-sectional profiles were provided by the Lithuanian Hydrometeorological Service, while additional data were obtained from Baltakis et al. [33]. All sources indicated that the river width exceeds the river depth by one to two orders of magnitude, allowing the hydraulic radius to be approximated by the flow depth.

2.3. Tritium Transport Modeling with GoldSim

Daily monitoring of ^{3}H concentrations in the Neris River at Vilnius revealed consistent deviations from natural background levels, suggesting a possible link to BelNPP operations. To assess the potential impact of BelNPP discharges on this region, it was necessary to estimate the volume and timing of ^{3}H releases. However, due to the unavailability of direct ^{3}H emission data from BelNPP during the study period, we developed a transport-decay model to support the indirect reconstruction of ^{3}H discharges. The core equation used for modeling transport and radioactive decay, i.e., Equation (1), is presented below:

$$\underbrace{\frac{\partial}{\partial t}{}^3H}_{\substack{\text{Time derivative}\\ \text{of tritium at any}\\ \text{observation point}}} = -\underbrace{\frac{\partial}{\partial x}u\cdot{}^3H}_{\substack{\text{Advective}\\ \text{transport of}\\ \text{tritium}}} + \underbrace{\frac{\partial^2}{\partial x^2}D\cdot{}^3H}_{\substack{\text{Diffusive}\\ \text{transport of}\\ \text{tritium}}} + \underbrace{W_{^3H}}_{\substack{\text{Diffuse sources}\\ \text{of tritium along}\\ \text{particular}\\ \text{river reaches}}} - \underbrace{k\cdot{}^3H}_{\substack{\text{Radioactive}\\ \text{decay of}\\ \text{tritium}}} \quad (1)$$

where ^3H is the tritium concentration [M·L^{-3}] (to be converted to BqL^{-1}), u is the river flow velocity [L·T^{-1}], D is the diffusive transport coefficient represented by the longitudinal dispersion in the river [L2·T^{-1}], and W_{H-3} is the diffuse influx of tritium per unit volume of the river in unit time [M·L^{-3}·T^{-1}] (to be converted to Bq time^{-1}), all considered to be functions of time (t [T]) and space (x [L]). k is the first-order decay constant [T^{-1}], which can be calculated using the half-time of tritium and is a constant in time and space since the radioactive decay is not affected by any environmental forcing such as temperature, pH, or even ingestion by the biota. Equation (1) describes the tritium concentration from any reference location (x = 0) as a function of time and location (for example, location x) along the river reach.

Any solution to Equation (1) that satisfies the initial and boundary conditions can be used to describe the combined effects of transport and radioactive decay, allowing for estimating tritium concentrations at any point in time and space under both current and future scenarios. However, obtaining an exact analytical solution is challenging due to the spatial and temporal variability in the functions $u(x,t)$, $D(x,t)$, and $W_{^3H}(x,t)$, as well as the complexity of accurately implementing initial and boundary conditions. Therefore, approximate numerical solutions are required in place of analytical approaches.

Using hydrographical data and the best available information on river cross-sections, it could be demonstrated that the diffusive transport of ^3H may be neglected in the case of the Neris River (Supplementary Material, Figure S1). Under this assumption, Equation (1) was simplified to Equation (2), which, although still difficult to solve analytically, was considerably easier for numerical implementation:

$$\frac{\partial}{\partial t}{}^3H(x,t) = -\frac{\partial}{\partial x}u(x,t)\cdot{}^3H(x,t) + W_{^3H}(x,t) - k\cdot{}^3H(x,t) \tag{2}$$

The numerical solution of Equation (2) required discretization in both time and space. For spatial discretization, the river was subdivided into a series of fully mixed volumes, conceptually represented as a feed-forward array of reactors with no feedback from downstream to upstream, forming the basis of a box model (Equation (3)). For the Neris River, this model consisted of 54 such boxes. For more convenient implementation, Equation (3) could be reformulated into a single matrix expression (Equation (4)), encompassing all 54 model boxes:

$$\frac{{}^3H_i^{t+\Delta t} - {}^3H_i^t}{\Delta t} = \frac{Q_{IN,i}^t}{V_i^t}\cdot{}^3H_{i-1}^t - \left(\frac{Q_{OUT,i}^t}{V_i^t} + k\right)\cdot{}^3H_i^t + {W_{^3H}}_i^t \tag{3}$$

$$\begin{bmatrix} {}^3H_1^{t+\Delta t} \\ {}^3H_2^{t+\Delta t} \\ {}^3H_3^{t+\Delta t} \\ \vdots \\ {}^3H_{52}^{t+\Delta t} \\ {}^3H_{53}^{t+\Delta t} \\ {}^3H_{54}^{t+\Delta t} \end{bmatrix} = \begin{bmatrix} {}^3H_1^t \\ {}^3H_2^t \\ {}^3H_3^t \\ \vdots \\ {}^3H_{52}^t \\ {}^3H_{53}^t \\ {}^3H_{54}^t \end{bmatrix} + \left(\begin{bmatrix} -\lambda_{1,1} & 0 & 0 & \dots & 0 & 0 & 0 \\ \phi_{2,1} & -\lambda_{2,2} & 0 & \dots & 0 & 0 & 0 \\ 0 & \phi_{3,2} & -\lambda_{3,3} & \dots & 0 & 0 & 0 \\ \vdots & \vdots & \vdots & \ddots & \vdots & \vdots & \vdots \\ 0 & 0 & 0 & \dots & -\lambda_{52,52} & 0 & 0 \\ 0 & 0 & 0 & \dots & \phi_{53,52} & -\lambda_{53,53} & 0 \\ 0 & 0 & 0 & \dots & 0 & \phi_{54,53} & -\lambda_{54,54} \end{bmatrix} \cdot \begin{bmatrix} {}^3H_1^t \\ {}^3H_2^t \\ {}^3H_3^t \\ \vdots \\ {}^3H_{52}^t \\ {}^3H_{53}^t \\ {}^3H_{54}^t \end{bmatrix} + \begin{bmatrix} \phi_{1,0}\cdot{}^3H_0^t + {W_{^3H}}_1^t \\ {W_{^3H}}_2^t \\ {W_{^3H}}_3^t \\ \vdots \\ {W_{^3H}}_{52}^t \\ {W_{^3H}}_{53}^t \\ {W_{^3H}}_{54}^t \end{bmatrix} \right) \cdot \Delta t \tag{4}$$

Here, i is the box index numbered from upstream to downstream, $Q_{IN,i}^t$ is the inflow into the box [L^3·T^{-1}], $Q_{OUT,i}^t$ is the outflow from the box, [L^3·T^{-1}], ${}^3H_i^{t+\Delta t}$ is the tritium concentration in the box [M·L^{-3}], V_i^t is the volume of the box [L^3], ${W_{^3H}}_i^t$ is the total tritium flux into the unit volume of the box excluding the upstream boxes [M·L^{-3}·T^{-1}], $-\lambda_{i,i}$

and $\phi_{i,i-1}$ are the diagonal and subdiagonal elements of the system matrix [T^{-1}] given in Equations (5) and (6), and ${}^3H_0^t$ is the upstream boundary concentration of tritium.

$$\phi_{i,i-1} = \frac{Q_{IN,i}^t}{V_i^t} \tag{5}$$

$$\lambda_{i,i} = \frac{Q_{OUT,i}^t}{V_i^t} + k \tag{6}$$

The derivation of Equations (3) and (4) from Equation (2) is provided in (Supplementary Material, Equations S19 to S50). As shown in Equation (3), the time discretization follows an explicit scheme, while the spatial discretization is based on an upwind approach. A simplified sketch of the spatial discretization is presented in Figure 2, and a more detailed schematic, depicting model boxes as control volumes with associated fluxes, is available in the Supplementary Material, Figure S2.

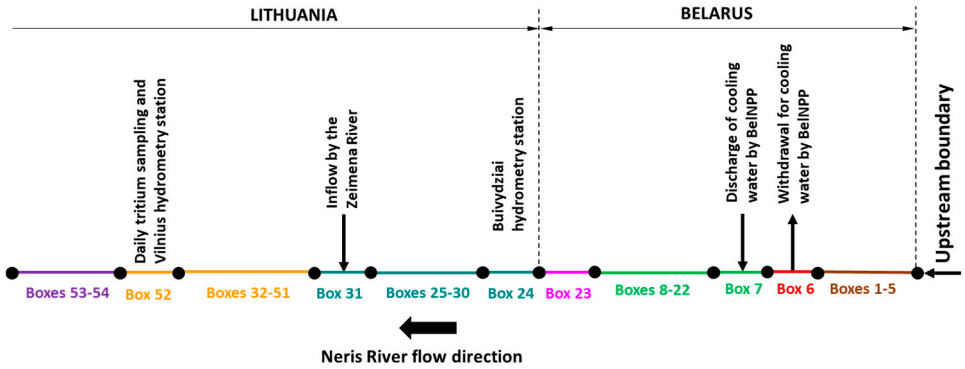

Figure 2. The model setup. Colors denote distinct hydraulic attributes across the discretized river boxes.

Based on the structure of the model equations, the implementation of the transport–decay model required a system dynamics approach, best suited for computational platforms that support dynamic feedback and time-stepping schemes. Two primary options were available for model implementation:

- Programming-based implementation using languages such as Fortran, R, Python, or MATLAB/Octave, which offer flexibility but require detailed manual coding and debugging;
- System dynamics modeling software, including next-generation tools such as OpenModelica, Vensim, Powersim, Stella, AnyLogic, or GoldSim, which are specifically designed for simulating time-dependent processes and allow for a modular, visually intuitive framework.

The latter approach—using a system dynamics modeling platform—was selected to enable more rapid model development and intuitive visualization. While most modern system dynamics tools could be used for this type of study, each is optimized for different application domains. For instance, OpenModelica, a graphical environment for the Modelica language [34], was excluded due to its relatively steep learning curve compared to other system dynamics platforms. Powersim [35] and AnyLogic [36] are primarily tailored to business and industrial modeling. Vensim is a general-purpose tool, while Stella is more frequently applied in environmental contexts.

GoldSim (Version 14) was ultimately selected for the following reasons:

- Environmental specialization: It includes built-in objects specifically designed for environmental applications, enabling streamlined modeling of contaminant transport and decay processes;
- Extensive prior use: GoldSim has been successfully applied for over two decades in studies related to environmental systems and public health [37,38], including numerous studies related to radionuclide transport [39–47];
- Flexibility and interoperability: The platform supports the use of user-developed libraries [48], allows for integration with external models [49], and can interface with other programming environments [50];
- Benchmarking: GoldSim has been benchmarked against other numerical tools, with demonstrated accuracy and consistency [51,52].

The model equations require several key inputs, including river geometry, estimates of flow depth for calculating box volumes, and discharge values along the model reach. These were derived by incorporating the Muskingum–Cunge method for hydrological routing [53], which uses river cross-sectional data to determine the two coefficients of the original Muskingum scheme. In this study, a hydrological model in the classical sense was not devised since the flows in the river were monitored by the Lithuanian Hydrometeorology Service. The Muskingum–Cunge method was mainly applied to estimate the flow-related properties of the Neris River (depth and flow velocity) needed for the transport model. Hydrological routing was preferred over a more detailed hydraulic or hydrodynamic routing method since there was not sufficient river cross-section information covering all of the domain of the transport model. As noted in Section 2.3, due to the wide and relatively shallow cross-section of the Neris River, the hydraulic radius was approximated by flow depth, simplifying the application of the Muskingum–Cunge method.

Since lateral inflows along the river also contain tritium—at least at background levels—their contributions were accounted for following the approach described by HEC [54]. As no explicit time series data for these diffuse inflows were available, they were reconstructed based on hydrological and catchment characteristics.

To reconstruct the lateral inflows for each model box, drainage areas were delineated for grouped boxes (Boxes 1–5, 6, 7, 8–22, 23, 24, 25–30, 31, 32–51, 52, and 53–54) using the automatic watershed delineation tool in ESRI's ArcGIS (Figure 3). The topographic data were obtained from the Shuttle Radar Topography Mission (SRTM), with a spatial resolution of 90 × 90 m at the equator (approximately 64 × 64 m at the Neris River's latitude) and a vertical accuracy of 1 m.

Upstream boundary flows and lateral inflows were calculated using daily discharge data provided by the Lithuanian Hydrometeorological Service, as described in Section 2.3. A constant water yield was assumed upstream of each hydrometric station, and upstream drainage areas were subdivided into sub-watersheds matching the box groups in Figure 3. Lateral flows were estimated using a water mass balance approach and proportionally distributed among boxes within each group according to box length. As daily values were needed, a dedicated infrastructure was built into the GoldSim model to perform these calculations automatically.

To simulate the downstream transport of tritium in the Neris River, a dynamic mass transport model was developed using GoldSim software (GoldSim Technology Group LLC). The model was structured to represent one-dimensional advection and radioactive decay processes within the river channel, with additional components to account for dilution and dispersion.

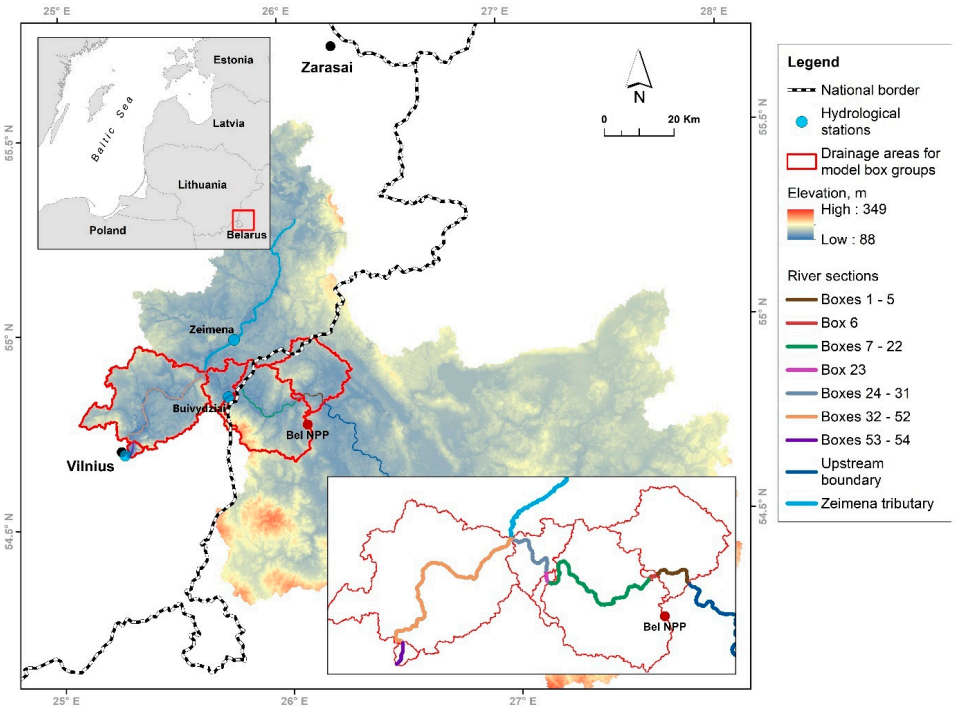

Figure 3. Delineation of drainage areas for model box groups. Map was produced using ArcGIS for illustrative purposes only.

Key input parameters included the following:

- ^{3}H discharge estimates from the BelNPP (approximated from observed concentrations at the border site);
- River flow velocity and cross-sectional area (estimated from available hydrological data);
- ^{3}H half-life (4500 days);
- Travel time between the two sampling sites.

The model was calibrated using observed ^{3}H concentrations at both monitoring sites and validated by comparing model outputs with independent measurements collected over the study period. A sensitivity analysis was conducted to evaluate the effects of varying discharge rates and flow conditions on downstream ^{3}H concentrations. As a full description of the model exceeds the scope of this manuscript, a read-only version is provided as an additional Supplementary Materials and can be accessed via Zenodo at https://doi.org/10.5281/zenodo.15647271 [55].

3. Results

3.1. Observed Tritium Concentrations—Experimental Approach

Time series of ^{3}H in monthly precipitation are essential for estimating the residence time of water in shallow aquifers in classical isotope hydrology studies. However, in our study, time series of ^{3}H in monthly precipitation is used as one of the methods for estimating the excess of ^{3}H in the river catchment area adjacent to the BelNPP. Data on ^{3}H content in precipitation in eastern Lithuania from two stations—Zarasai and Vilnius—have been available since 1999 and 2017, respectively (Figure 4).

A comparison of ^{3}H data for the Zarasai station with those of the well-known Vienna GNIP station for the overlapping period yielded a correlation of 0.72 [14], supporting the use of earlier Vienna data to plausibly reconstruct ^{3}H values prior to the beginning of observation in our region. According to global data [56], the ^{3}H content in atmospheric precipitation has been steadily decreasing since the era of thermonuclear weapons testing

in the 1950s and 1960s, approaching levels associated with natural cosmogenic production by around 2000.

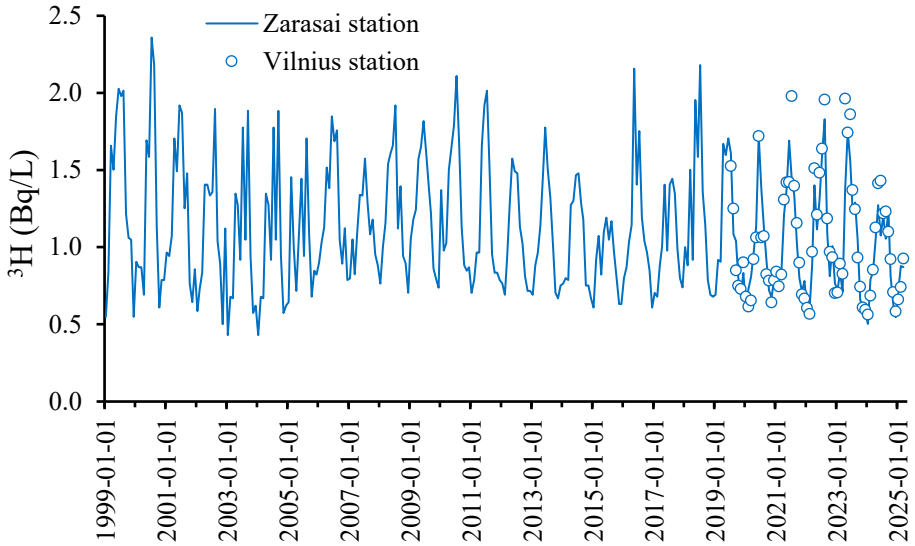

Figure 4. Activity concentration of ^{3}H in monthly precipitation in eastern Lithuania during 1999–2025 [14]. The Zarasai and Vilnius stations began operation in 1999 and 2017, respectively. For the overlapping period, the datasets from both stations show a strong linear correlation, described by the equation $y = 1.0676x - 0.0372$ with $R^2 = 0.8548$.

In particular, from 1999 to the end of 2024, the long-term mean ^{3}H activity concentration in precipitation at the Zarasai station ± standard deviation (SD) was 1.10 ± 0.40 Bq/L. Very similar ^{3}H variations were observed since 2017 at the Vilnius station, which is located closer to the BelNPP site than Zarasai. However, both ^{3}H datasets show strong agreement, with a correlation of 0.92 for the overlapping period of 2017–2024. During this period, the long-term mean ^{3}H activity concentration in precipitation at Vilnius was 1.00 ± 0.40 Bq/L, with a minimum of 0.56 ± 0.04 Bq/L (1σ total uncertainty of a single measurement) and a maximum of 2.00 ± 0.13 Bq/L (1σ). The current level of ^{3}H in precipitation was mainly attributed to cosmogenic production, exhibiting a pronounced seasonal cycle with lower values in winter (October–February) and higher values in summer (May–August).

Further analysis presented below shows that prior to the commissioning of the BelNPP, the ^{3}H concentrations in the Neris River during summer were typically 2–3 times lower than those observed in summer precipitation samples, while in winter, river water ^{3}H levels were almost equal to or slightly lower (up to 1.5 times) than those in winter precipitation. Based on these observations, the background (baseline) ^{3}H concentration in Neris River water during the operational period of the BelNPP is presented in Figure 5.

From 2019 to the end of 2024, the mean ^{3}H activity concentration in winter precipitation at the Vilnius station was 0.75 ± 0.12 Bq/L (±SD).

Another approach for determining the ^{3}H background level in the Neris River was based on integrating three datasets: (1) ^{3}H data from the Neris River during the pre-commissioning period (2017–2020), (2) background ^{3}H data from the Zeimena River—the main tributary in the study area—during the operational period of the BelNPP (2024–2025), and (3) a subset of minimum ^{3}H values from the Neris River itself during the operational period (2020–2023) (Figure 6).

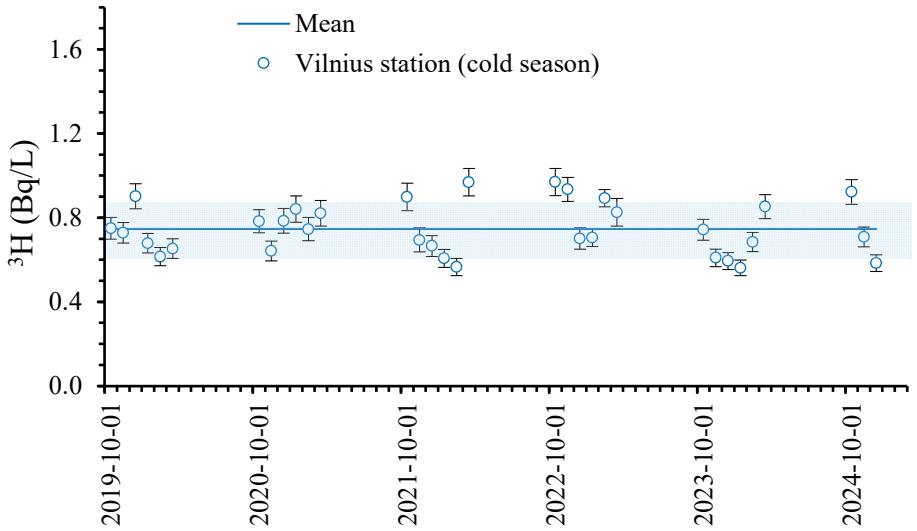

Figure 5. Monthly ^{3}H activity concentration in precipitation during the cold season (October-March) at the Vilnius station in 2019–2024. Error bars indicate uncertainties of a single measurement (1 sigma). The solid line indicates the mean ^{3}H activity concentration, with ±1 standard deviation.

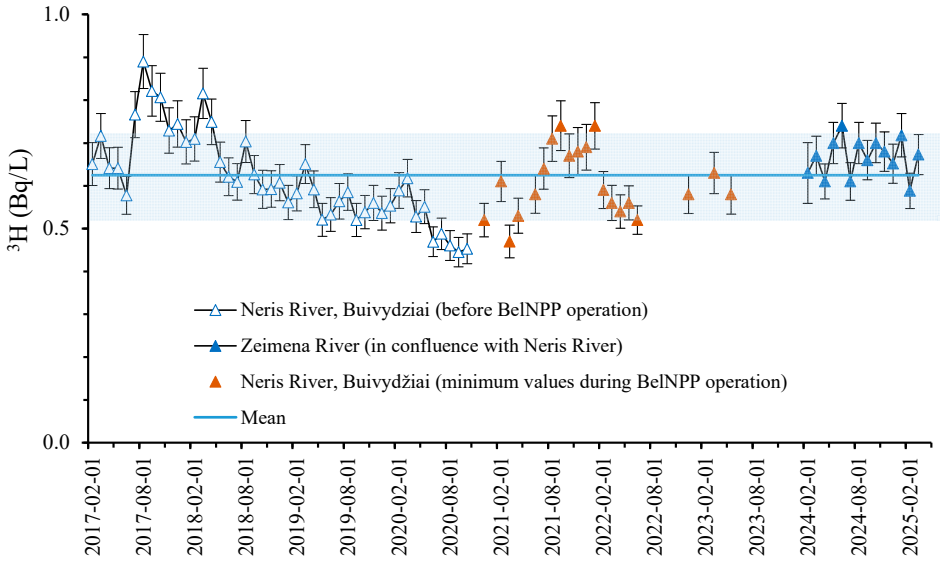

Figure 6. ^{3}H activity concentration in the water of the Neris and Zeimena Rivers during 2017–2025. The three datasets shown were used to estimate the background ^{3}H levels in the Neris River during the initial operational period of the BelNPP. Error bars indicate uncertainties of a single measurement (1 sigma). The solid line indicates the mean ^{3}H activity concentration, with ±1 standard deviation.

The long-term mean ^{3}H concentration, taken as the background value based on three sets of river water samples from the Neris River in the study area, is 0.62 ± 0.09 Bq/L (±SD), with a minimum of 0.45 ± 0.03 Bq/L (1σ) and a maximum of 0.89 ± 0.06 Bq/L (1σ). This range is very similar to the ^{3}H background concentrations derived from cold-season precipitation data. The slightly lower background levels observed in river water compared to precipitation may reflect a delayed signal transmission due to baseflow contributions, which typically exhibit residence times of approximately 3–4 years.

The smoothing of the seasonal ^{3}H variations in the Neris River before the commissioning of the BelNPP is attributed to mixing and storage processes, including baseflow primarily formed from autumn and winter precipitation. Nevertheless, small peaks in ^{3}H activity can be observed—most commonly in March and August—against a general background of gradually decreasing ^{3}H levels over several years. This slight long-term

decrease may be explained by the continued release of ^{3}H from older water stored in the catchment, originating from precipitation events with increased ^{3}H concentrations during the era of thermonuclear weapons testing.

The specific activity of ^{3}H in the water of the Neris River at the border site—located approximately 34 km downstream from the BelNPP—for the period 2017–2025 is presented in Figure 7.

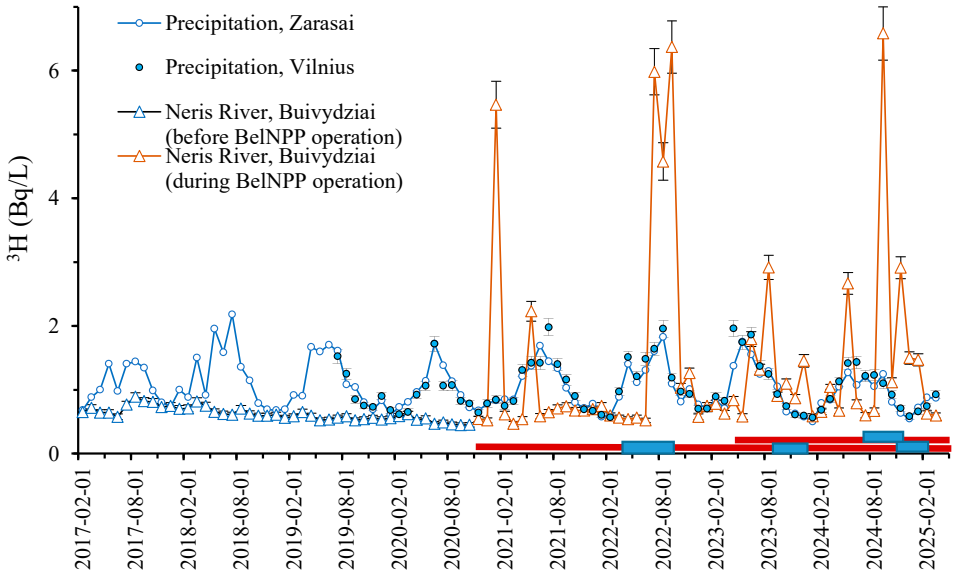

Figure 7. Activity concentrations of ^{3}H in atmospheric precipitation at the Zarasai and Vilnius stations and in surface water of the Neris River at the border site (Buivydziai) during 2017–2025. Red bold lines indicate the operational periods of the BelNPP; blue bands indicate the scheduled preventive maintenance periods—three for Unit 1 and one for Unit 2. Error bars indicate uncertainties of a single measurement (1 sigma).

Based on monthly sampling frequency, multiple distinct peaks of ^{3}H activity in the Neris River water were recorded during the operational period of the BelNPP. The most pronounced peaks were observed on 15 January 2021 (5.47 ± 0.37 Bq/L; 45.9 ± 3.1 TU), 15 September 2022 (6.37 ± 0.41 Bq/L; 53.4 ± 3.4 TU), and 13 September 2024 (6.58 ± 0.42 Bq/L; 55.2 ± 3.5 TU). In each of these cases, the tritium activity in the river water exceeded that in atmospheric precipitation for the corresponding month by approximately 6.5, 5.4, and 6.0 times, respectively. These peaks indicate episodic increases in ^{3}H input to the river system, potentially associated with operational or maintenance-related discharges from the BelNPP.

Therefore, considering the previously noted ^{3}H variations based on monthly sampling, the need arose to determine more precise short-term fluctuations in ^{3}H levels in the Neris River. For this purpose, daily sampling was carried out at the Vilnius sampling site, allowing for a more detailed assessment of tritium dynamics in the river (Figure 8).

Based on the daily sampling frequency in 2023, significantly more pronounced ^{3}H peaks were observed in the water of the Neris River compared to the monthly data shown in Figure 7. The highest peaks recorded were on 26 January (20.49 ± 0.61 Bq/L (171.9 ± 5.1 TU)), 10 July (11.14 ± 0.46 Bq/L (93.5 ± 3.9 TU)), and 17 December (26.25 ± 0.68 Bq/L (220.2 ± 5.7 TU)).

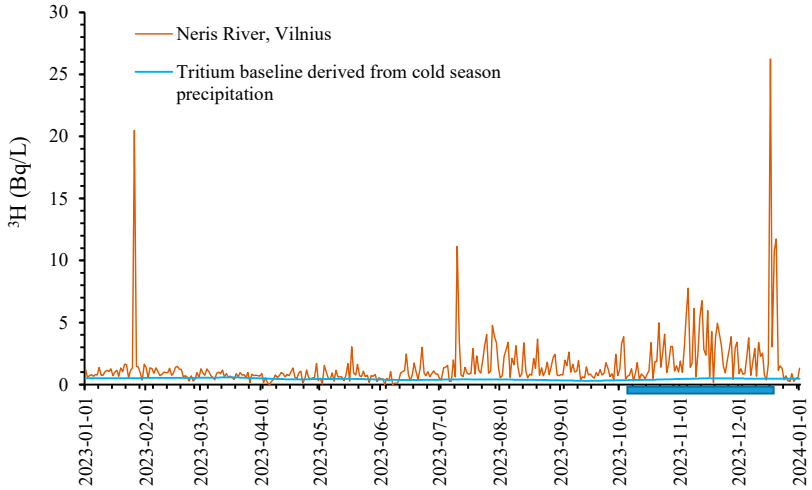

Figure 8. The daily ^{3}H activity concentrations in the water of the Neris River at the Vilnius site in 2023. The blue strip shows the period of scheduled preventive maintenance for Unit 1 of the BelNPP.

3.2. Modeling Results

The model provides two primary outputs: river hydrology parameters (such as water depths and flow velocities) and ^{3}H concentrations. Its operation consists of two main steps: first, reproducing the river's hydrological characteristics, and second, generating the ^{3}H input datasets—namely concentrations at the upstream boundary and in lateral inflows—required to run the transport model.

3.2.1. The Hydrographic Results

The hydrographic results were obtained through a standard model calibration procedure, in which the flow rates predicted by the model's hydrological components were compared to the observed flow rates recorded at the gauging stations described in Section 2.3. Calibration was performed by adjusting Manning's roughness coefficients until the simulated flow rates closely matched the measured data.

The idea here is not to calibrate and validate a process-based hydrological model. As stated in Section 2, the upstream and lateral flows for the transport model domain that would be generated by a rainfall–runoff model in case of the absence of necessary flow information are already estimated with desired accuracy considering the aims of this study. The only question left here is if the flow rates monitored at the downstream hydrometeorological site can be reproduced with high accuracy. This is important since there are no hydrographic monitoring stations measuring the flow properties (depth and velocity) desired for the ^{3}H transport model. The travel time in the river should be reproduced as correctly as possible. This can only be achieved with correctly estimated flow velocity. The correctness of the estimated flow velocity can only be checked with a calculated flow hydrograph that fits the real hydrographs as perfectly as possible.

As seen in Figure 9, the calculated flow rates have excellent agreement with the monitored flow rates, with a high coefficient of determination (R^2) exceeding 0.99 for both hydrometry stations. The relative errors (REs) were low, calculated as 0.39% for Buivydziai and 0.67% for Vilnius, with corresponding percent biases (PBIASs) of −0.0081% (practically 0) and 0.13%, respectively. Another important performance metric, the Nash–Sutcliffe model efficiency coefficient (NSE), introduced by Nash and Sutcliffe [57], also indicated strong model performance, with values exceeding 0.99 for both stations. This may look like an overfit in the case of a general process-based hydrological model, but it was intentionally performed in this manner based on the needs described in the previous paragraph.

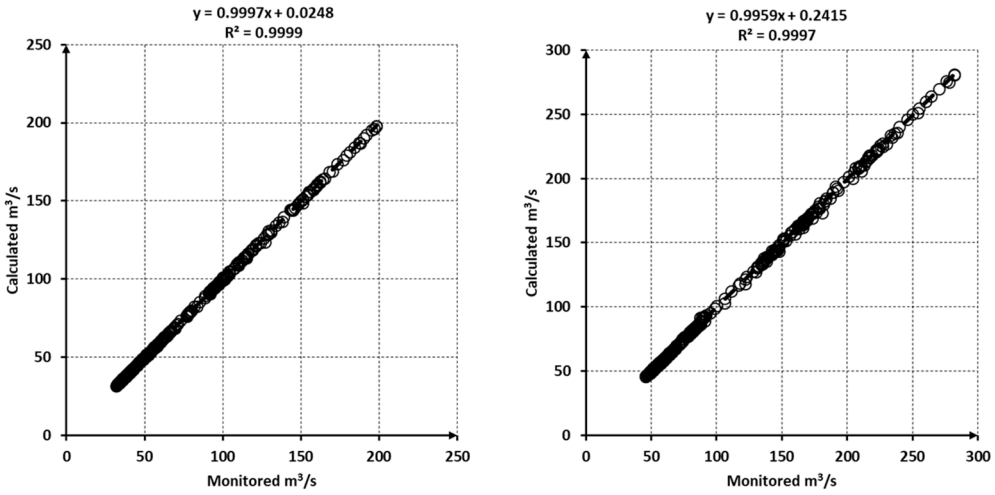

(**a**) (**b**)

Figure 9. A comparison of monitored and model-calculated flow rates for 2023: (**a**) Buivydziai hydrometry station; (**b**) Vilnius hydrometry station.

We, therefore, conclude that the hydrographic components of the model are well calibrated and capable of reproducing other hydrographic outputs, such as water velocity, depth, and volume, for each of the transport model box shown in Figure 2. These outputs can be directly utilized in the tritium transport model. Further discussion of the hydrographic modeling results is presented in Section 4.2.

Another output of the hydraulic calculations is the flow lag time between the BelNPP and Vilnius. This lag time is defined as the cumulative flushing time—calculated as the ratio of box volume to outflow rate—for each model box from the BelNPP discharge location (Box 7) to the daily tritium sampling site in Vilnius (Box 52). Lag times were computed by running the hydrographic components of the model from 2018 to 2023 (6 years) and are presented as monthly box plots in Figure 10.

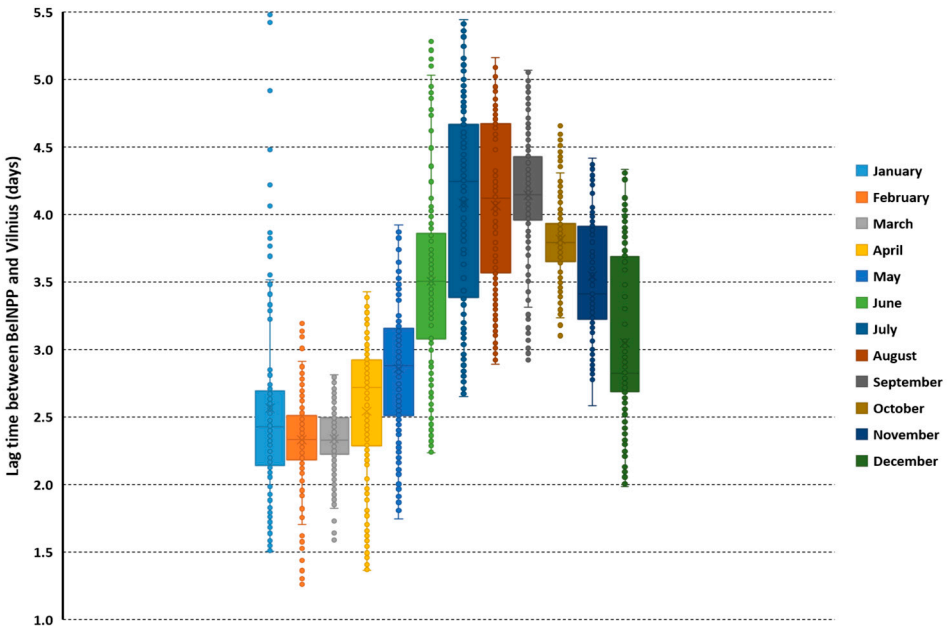

Figure 10. The lag time between the BelNPP (Box 7) and Vilnius (Box 52), calculated for 2018–2023 using the hydrographic components of the model. The results are presented as monthly box plots.

The lag time presented in Figure 10 clearly demonstrates that the time delay—typically a few days—between the BelNPP and Vilnius is negligible compared to the half-life of tritium, which is approximately 4500 days. Therefore, in this study, tritium is treated as a conservative tracer, whose radioactive decay between the BelNPP and Vilnius can be reasonably neglected. Given this, the lag time results shown in Figure 11 may also be applicable for assessing the fate of other water-soluble isotopes potentially released during accidental events, as well as for evaluating associated risks to the Neris River ecosystem. In this study, a daily time series of lag time values was required to reconstruct the possible tritium discharge concentrations from the BelNPP through inverse modeling. This daily time series, covering the monitoring period in Vilnius, is shown in Figure 11.

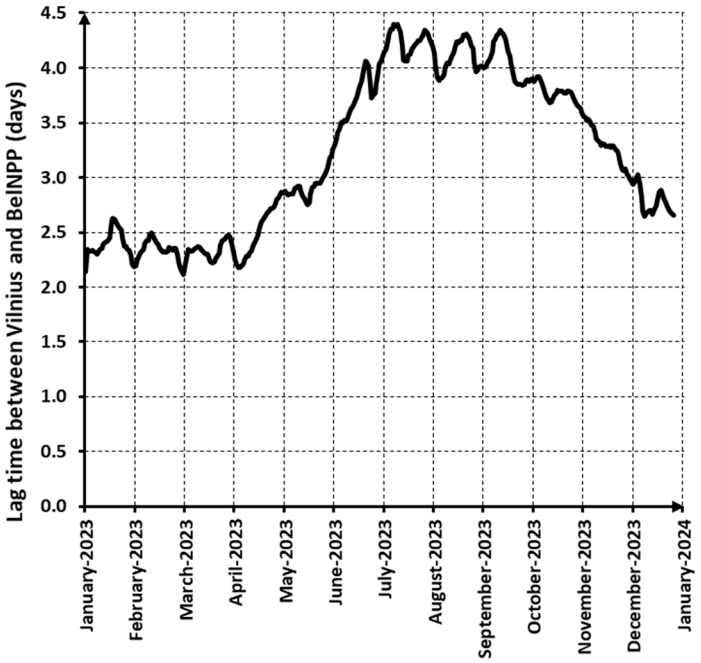

Figure 11. Daily lag time series between the BelNPP and Vilnius during 2023.

3.2.2. Results of Reconstructed Tritium Discharges from the BelNPP

In this study, it was assumed that the BelNPP is the primary source of deviations from the background tritium concentration (i.e., measured ^{3}H minus background ^{3}H) observed at the Vilnius sampling station on the Neris River. The daily excess activity of tritium (in Bq/day), attributable to the BelNPP discharges, was calculated by multiplying the river flow rate by the difference between the measured and background tritium concentrations. By applying a time lag correction to account for the travel time between the BelNPP and Vilnius (as established in Section 3.2.1), the estimated time series of discharged ^{3}H activity from the BelNPP is determined, and it is presented in Figure 12.

To evaluate the validity of the reconstructed ^{3}H discharge activity from the BelNPP, we used the tritium transport model incorporating the time series shown in Figure 12. This dataset was included alongside the river hydrography and background ^{3}H activity from upstream and lateral inflows. If the modeled daily tritium concentrations closely match the observed daily monitoring data, the reliability of the reconstructed discharge time series would be supported. The model outputs were compared with field measurements, and a regression analysis between observed and simulated values is presented in Figure 13. Additionally, box-and-whisker plots for each month were generated to provide a visual assessment of the model fit, confirming an adequate agreement between observed and modeled tritium concentrations (Figure 14).

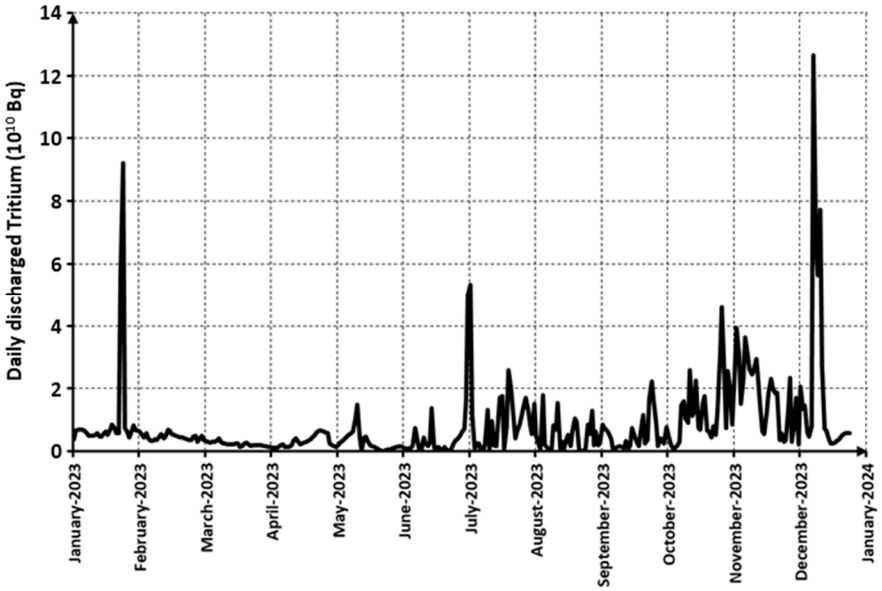

Figure 12. The reconstruction of daily discharged ^{3}H activity from the BelNPP during 2023.

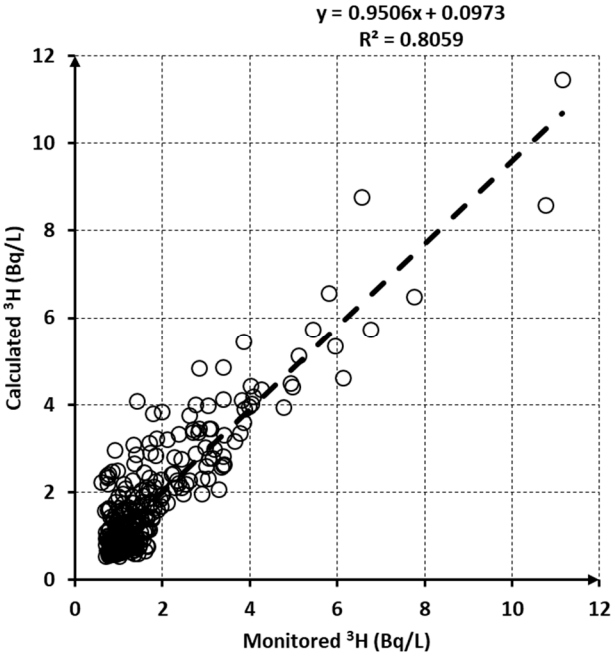

Figure 13. A comparison of monitored and model-calculated ^{3}H activity concentrations in the Neris River at Vilnius during 2023.

As seen in Figure 13, the model-calculated tritium activity concentrations show a reasonable correlation with the monitored values, with a coefficient of determination (R^2) of 0.8059, a relative error (RE) of 33%, a percent bias (PBIAS) of −2.87%, and a Nash–Sutcliffe model efficiency coefficient (NSE) of 0.61. PBIAS, RE, and NSE were calculated based on the mean value of the daily monitoring, where each sample was repeated three times. The monitoring results themselves have a relative uncertainty of ±30% based on random errors. Since RE and NSE are more affected by random errors, this uncertainty can explain a relative error of 33% and an NSE of 0.61, which can still be considered to present a moderate model performance.

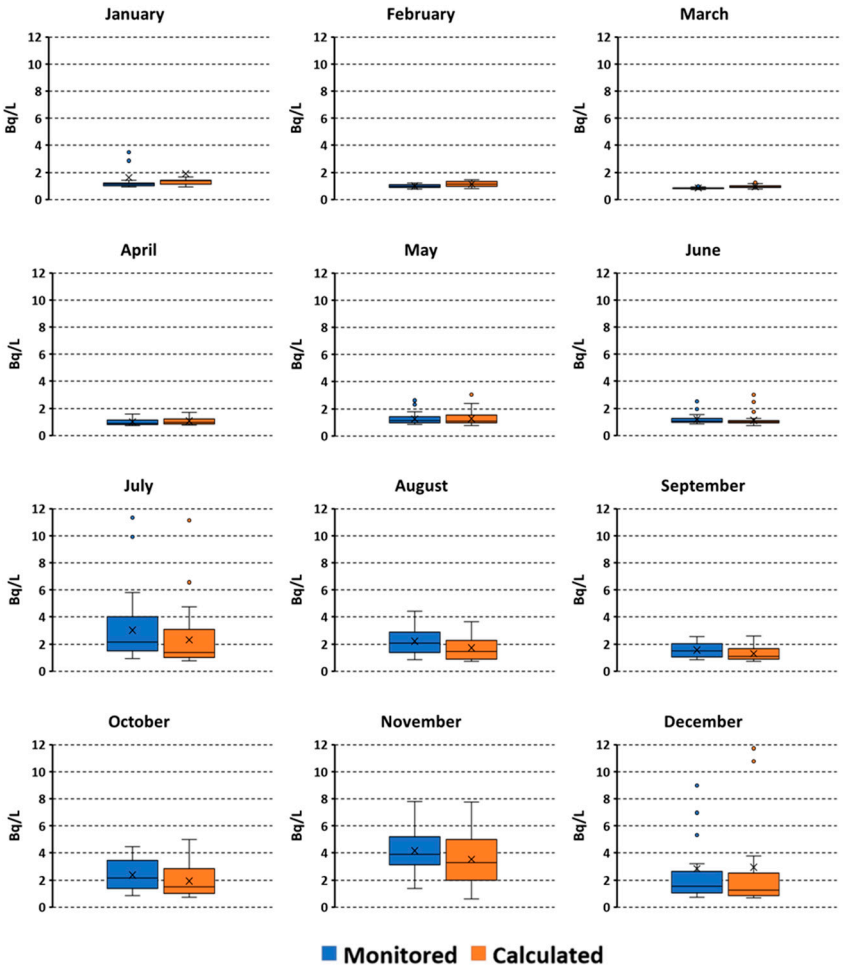

Figure 14. Monthly box-and-whisker plots comparing monitored and model-calculated ^{3}H activity concentrations at the Vilnius monitoring site.

Based on the integration of the ^{3}H transport modeling results for all of 2023, the reconstructed annual ^{3}H discharge from the BelNPP is estimated to be 2.95×10^{12} Bq, with a relative uncertainty of ±30%, including the contribution of ^{3}H monitoring.

4. Discussion

4.1. Interpretation of Observed Tritium Variations in the Context of BelNPP Operations

The BelNPP is the first nuclear power plant in Belarus, located in the catchment area of the transboundary Neris River. This has generated regional interest, particularly in Vilnius, which is located downstream. Already during the initial period of the BelNPP's operation, it was noted that increased ^{3}H activity in the Neris River occurred shortly after the plant was put into operation, with the first ^{3}H peak observed on 15 January 2021 (Figure 7). Longer-term observations have shown that higher ^{3}H activity tends to occur in liquid discharges during scheduled preventive maintenance periods—sometimes shortly before or after them. According to BelNPP reports (http://www.belaes.by [58]), the following preventive maintenance periods occurred: for Unit 1—25 April 2022 to 22 August 2022, 6 October 2023 to 19 December 2023, and 3 December 2024 to 27 January 2025; for Unit 2—26 July 2024 to 14 October 2024. Although ^{3}H emissions from nuclear power plants are generally within regulatory limits, detailed analysis of ^{3}H as a "fingerprint" of nuclear activity, especially in transboundary rivers, can provide a better understanding of the operational characteristics of a particular nuclear facility.

By subtracting the background ^{3}H data from the daily ^{3}H dataset for the Neris River in 2023, it was possible to estimate the ^{3}H excess resulting from the liquid discharges of the BelNPP, as presented in Figure 15.

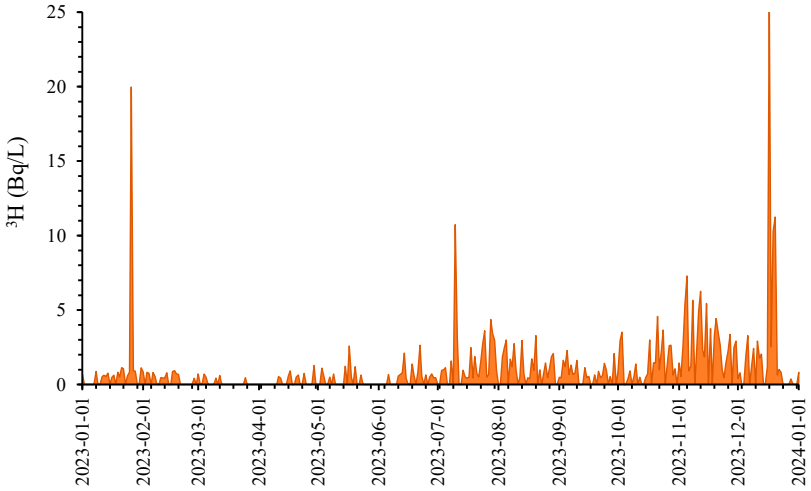

Figure 15. The daily ^{3}H excess in the water of the Neris River at the Vilnius site in 2023, attributed to liquid discharges from the BelNPP.

The maximum daily ^{3}H excess in 2023 (25.76 $\pm$ 0.72 Bq/L or 216.1 $\pm$ 6.0 TU) was observed following the completion of scheduled preventive maintenance at Unit 1 of the BelNPP. Nevertheless, the measured ^{3}H concentrations remained well below international regulatory limits; for instance, the World Health Organization (WHO) recommends a guideline value of 10,000 Bq/L for tritium in drinking water [59].

Daily sampling at the Vilnius site in 2023 (Figure 8) revealed more distinct and frequent ^{3}H peaks compared to monthly sampling. These high-resolution data indicate that short-term discharge events may go undetected under standard monthly monitoring, underscoring the importance of increased sampling frequency for accurately identifying and quantifying ^{3}H inputs. The results demonstrate that anthropogenic ^{3}H was present in the Neris River on most days of 2023. This finding enabled the estimation of the annual ^{3}H discharge in the order of 10^{12} Bq, which serves as a valuable input for subsequent modeling of tritium transport in the river system. The magnitude of the annual ^{3}H discharge from the BelNPP is comparable to values reported for many European nuclear power plants [60].

4.2. Model Reliability and Limitations

As previously stated, the model consists of two main components: a hydrological routing component, which performs flow routing calculations and estimates lateral inflows for each model box, and a tritium transport component, which solves the advection–reaction equation. In this case, the reaction term—^{3}H radioactive decay—is much less significant than the advection component.

The hydrological routing component successfully produced results related to river flow and lag times. The adequacy of these results for use in the tritium transport component was assessed by comparing the daily monitored and simulated flow rates. As reported in Section 3.2.1, four commonly used model performance metrics were applied: the coefficient of determination (R^2), the relative error (RE), the percent bias (PBIAS), and the Nash–Sutcliffe model efficiency coefficient (NSE). Given that the hydrological routing component functions similarly to a standard hydrological model, established performance benchmarks from the literature, such as those reported by Moriasi et al. [61], Ritter and Muñoz-Carpena [62], and Moriasi et al. [63], were used for evaluation.

According to these benchmarks, the model's performance falls into the "very good" category with respect to NSE and PBIAS. In addition, the RE values, being very close to 0, indicate that the hydrological routing procedure neither overestimates nor underestimates the flow rates at either of the gauging stations. The R^2 value exceeding 0.99 suggests that the model is adept at explaining nearly all of the variability in river flow data.

Taken together, these metrics suggest that the hydraulic calculation results have negligible uncertainty. This is an important consideration, as these hydrographic outputs serve as inputs to the tritium transport model, which itself is subject to other sources of uncertainty. Consequently, the contribution of hydrographic uncertainties to the overall uncertainty in tritium transport modeling can be considered minimal, thus simplifying subsequent uncertainty interpretation.

The transport model demonstrated a relatively lower goodness of fit compared to the hydrological routing component, with the most pronounced discrepancy observed in the relative error (RE). Although an RE of 33% may appear substantial, it is important to note that the average coefficient of variation (defined as the ratio of standard deviation to mean) in the monitored tritium data was 0.57 (57%). This high variability suggests that the relative error could have been largely attributed to the inherent noise in the observational data, assuming that the errors are random in nature.

Furthermore, the percent bias (PBIAS) was calculated as −2.87%, which is an order of magnitude smaller than the RE. This implies that the majority of the deviations between the modeled and observed values are compensatory in nature, with a slight tendency toward underestimation. Such a result supports the interpretation that the error is predominantly random rather than systematic.

Unlike hydrological modeling, standardized benchmarks for goodness of fit in water quality transport modeling are less well established. Nevertheless, some relevant references exist. For instance, Fernandes et al. [64] consider PBIAS values within ±10% to indicate high model performance. In this context, the PBIAS of ~3% obtained in our model is well within the acceptable range. Similarly, Jung et al. [65] reported ranges of 0.31–0.85 for R^2 and 0.33–0.87 for NSE in comparable studies. The values achieved in this study—0.8059 for R^2 and 0.61 for NSE—are consistent with those reported in the literature and suggest that the tritium transport model performs with adequate accuracy for the intended application. Considering that the hydrographic calculation results are highly accurate from a hydrological modeling perspective, thus contributing minimally to overall uncertainty, and that diffusive processes in the Neris River, which could otherwise be significant sources of uncertainty, are negligible (Supplementary Material, Figure S1) the primary remaining sources of uncertainty are the BelNPP-discharged tritium (Figure 12) and the background tritium concentrations. The degree of uncertainty can be estimated using the coefficient of determination (R^2 = 0.8059), which indicates that approximately 80% of the variability in tritium concentrations observed at the Vilnius monitoring site is explained by the model developed in this study, while the remaining 20% can be attributed to unexplained variability and associated uncertainty.

Like any model related to aquatic ecosystems, the one developed in this study also has its limitations:

- The model was developed as a prototype within the system dynamics simulation environment GoldSim rather than as stand-alone software. This decision was made to ensure the shortest possible development time. Although GoldSim is one of the most flexible system dynamics platforms and the model was designed using its built-in elements in a way that allows for further modification by other users, it remains less universal than a fully stand-alone product. In other words, some adjustments to the model will be necessary to apply it to other, similar problems.

- The transport model does not include diffusive transport processes and, therefore, does not account for longitudinal dispersion in the river. As previously noted, this decision was based on the hydrographic characteristics of the Neris River and the slow decay rate of ^{3}H, both of which result in low estuary numbers, indicating that advection is the dominant process. While this simplification facilitates model development in any simulation environment, it limits the applicability of the model to rivers with relatively faster flow or to radionuclides with slower decay rates. Nevertheless, users may modify the transport model to incorporate longitudinal dispersion into the numerical solution algorithm. This addition is of moderate complexity and would require a reasonable investment of time and effort. Alternatively, users may apply the cell-link transport features provided by the radionuclide version of the GoldSim Contaminant Transport Module.
- The model is designed to simulate only the main river branch and does not explicitly include tributaries along their flow paths. This limitation can be addressed in two ways. The first option is to restructure the model so that multiple instances can be executed sequentially in an upstream-to-downstream manner, with the material flux at the downstream end of each reach serving as the upstream or tributary input for the next reach. This approach is feasible as long as diffusive transport processes are excluded, as performed in this study. The second option is to incorporate the tributaries directly into the model domain, which would require rewriting the entire numerical solution framework—either using standard GoldSim elements or the radionuclide version of the GoldSim Contaminant Transport Module. This approach allows for including diffusive processes but would require substantially more development effort.
- The model is designed for radionuclides that exist in dissolved form in water. It does not account for adsorption onto particles, settling into sediments, sedimentary processes, other stunting mechanisms, or interactions with biota.

4.3. Comparison with Other River Systems Affected by Nuclear Facilities

When comparing the findings of this study with those from other rivers affected by liquid discharges from nuclear facilities, generally similar trends can be observed. It is well established that no effective technology currently exists for removing tritium from nuclear power plant (NPP) effluents, making it a common component of liquid radioactive discharges [66]. In light of this, several rivers—some of which have also been analyzed using transport models comparable to the one employed in this study—were briefly compared with the Neris River.

The Rhône River, the principal river flowing into the western Mediterranean in France, is notable for its high concentration of nuclear-related facilities. These include 4 nuclear power plants (NPPs) comprising 14 reactors, as well as two major nuclear sites hosting both civilian and military operations [66]. Downstream tritium concentrations in the Rhône have been reported to reach values up to five times higher than those observed upstream. According to Eyrolle et al. [67] and Boderau et al. [68], typical tritium concentrations range from 1.0 ± 0.7 to 61.5 ± 2.7 Bq/L (mean: 6.0 Bq/L) and from 1.2 ± 0.1 to 13.9 ± 1.4 Bq/L (mean: 5.3 Bq/L), respectively. These levels are of the same order of magnitude as those observed in our monitoring of the Neris River at Vilnius.

The Loire River, also located in France and encompassing 14 NPPs within its watershed, is among the most extensively studied rivers in terms of tritium contamination. This river system has been investigated through both intensive monitoring campaigns and modeling approaches similar to the one developed in this study. Siclet et al. [69] and Goutal et al. [70] applied a one-dimensional transport model to simulate tritium behavior in the Loire. Goutal et al. [70] reported the correlation coefficient (r) as an indicator of

model fit; when recalculated as the coefficient of determination (R^2), this corresponds to a value of approximately 0.61—slightly lower than but still comparable to that obtained in our study. More recently, Sizonenko and Sinitsyn [71] applied another one-dimensional transport model to the Loire River, using a numerical solution technique similar to ours, where the river is represented as a series of continuously stirred control volumes. Tritium concentrations reported in these studies were generally higher than those observed in the Neris River, though still of the same order of magnitude.

Pujol and Sanchez-Cabeza [72] investigated the Ebro River in Spain and highlighted that, during normal operation, the associated nuclear power plant discharges low-activity radioactive liquid waste, including tritium, into the river in a controlled manner. As a result, the tritium concentrations observed in the Ebro River were relatively low and comparable to those measured in the Neris River.

The Tagus River, which flows through Spain and Portugal, has also been studied for its tritium content in relation to discharges from nearby nuclear power plants. Baeza et al. [73] and Baeza et al. [74] reported slightly higher tritium concentrations in the Tagus River compared to the Neris River. Nevertheless, the downstream tritium levels observed in the Tagus River were of the same order of magnitude as those found in the Neris River. Notably, Baeza et al. [74] applied a tritium transport model similar in structure to the one developed in this study.

The Sava and Danube Rivers, particularly where they flow through Serbia and Croatia, exhibit tritium concentrations generally similar to those observed in the Neris River, as reported by Grahek et al. [75]. Both rivers receive discharges from nuclear power plants, and some of the observed deviations in tritium levels from background concentrations can be attributed to the declining influence of atmospheric fallout from nuclear weapons testing. Notably, the peak in tritium activity resulting from such fallout occurred in 1963 [3,75].

However, not all rivers that are comparable to the Neris River in terms of receiving NPP discharges exhibit similar tritium concentrations. The Jihlava and Vltava Rivers, located in the Czech Republic and Slovakia, are also impacted by discharges from nuclear power plants, as well as residual contamination from atmospheric nuclear weapons tests and the Chernobyl disaster. Studies by Hanslik et al. [76], Hanslik et al. [77], Simek et al. [78], and Hanslik et al. [79] indicate that tritium concentrations in these rivers are nearly an order of magnitude higher than those observed in the Neris River. This may be partly due to the fact that, unlike the typical practice of discharging NPP effluents into large rivers, these particular rivers are smaller watercourses [76,77]. Additionally, Panov et al. [80] reported cases in which downstream tritium concentrations were up to 36 times higher than upstream levels.

4.4. Implications for Transboundary Water Management and for Further Studies

This study was conducted to investigate tritium dynamics and highlight the importance of accurate long-term isotopic monitoring in addressing broader environmental challenges and assessing the impacts of nuclear facilities on ecosystems and human health. The findings emphasize the value of high-frequency isotopic observations in environments affected by nuclear installations located near transboundary aquatic systems. Using tritium as a tracer or fingerprint provides critical insight into regional environmental sustainability and facilitates evidence-based management of shared water resources.

The obtained results suggest directions for extending future studies, both in terms of experimental research and the expansion of modeling approaches. The current system of experiments and modeling related to tritium should be broadened to include a biotic component. Furthermore, after appropriate development, the model could be adapted to simulate other mobile radionuclides such as carbon-14 and iodine-131. Preliminary

experimental data already indicate detectable levels of carbon-14 attributable to the BelNPP. The inclusion of radionuclides such as cesium-137 and cobalt-60—substances subject to sorption processes and transport with suspended matter in the river system—would require the greatest possible effort in both experimental and modeling research.

It is also evident that international cooperation is essential for ensuring that science-based assessments of environmental conditions, particularly in transboundary waters, are conducted in a timely and effective manner for the benefit of the public.

5. Conclusions

The following conclusions were reached during this study:

- Long-term, high-frequency measurements of tritium concentrations in the Neris River near the Belarus–Lithuania border and in Vilnius have revealed elevated tritium levels compared to background, with greater variability observed since the Belarusian Nuclear Power Plant (BelNPP) began operations.
- This excess tritium is attributed to routine discharges from the BelNPP, with the estimated annual tritium release reaching approximately $2.95 \cdot 10^{12}$ Bq. Observed fluctuations in tritium concentrations correspond closely with the operational schedule of the facility, particularly during and around scheduled maintenance periods. Comparisons with other river systems impacted by NPPs suggest that the tritium levels in the Neris River are within the typical range observed across Europe.
- A tritium transport model was developed to simulate the fate and timing of upstream discharges reaching downstream locations. The model provides insight into the lag time and magnitude of tritium transport under observed hydrological conditions.
- The model is adaptable to future applications, including the simulation of other water-soluble radionuclides, provided that isotope-specific parameters and hydrological data are available.
- Further studies are recommended for incorporating more complex environmental processes, including biogeochemical cycling, sediment interactions, and ecological impacts of other radionuclides. Such research would enhance our understanding of radionuclide behavior in transboundary aquatic systems.

Supplementary Materials: The following supporting information can be downloaded at: https://www.mdpi.com/article/10.3390/w17172580/s1: Tritium Transport in the Transboundary Neris River During the Routine Operation of the Belarusian Nuclear Power Plant: A Monitoring and Modeling Approach. A read-only supporting information can be accessed at https://doi.org/10.5281/zenodo.15647271. References [81–85] were cited in the supplementary material.

Author Contributions: The initial draft of this paper was written by all the authors; validation, supervision, resources, methodology, data curation J.M. and Ž.S.; methodology, data curation O.J., R.P. (Rimantas Petrošius), V.R. and B.A.; model development, simulation A.E. and Ž.S.; project administration Ž.S. and R.P. (Ričardas Paškauskas); visualization V.R., J.M., A.E. and R.P. (Ričardas Paškauskas). All authors have read and agreed to the published version of the manuscript.

Funding: This research received no external funding.

Data Availability Statement: The data used to support this paper are available from the corresponding author upon request.

Acknowledgments: In preparing this manuscript, the authors used OpenAI to support language improvements. The input provided by the platform was subsequently subjected to a thorough review by the authors. The authors would like to express their sincere gratitude to Rita Linkeviciene for her assistance in supplying hydrological data and reference materials. The authors are grateful to the reviewers of this manuscript for their thoughtful and helpful comments.

Conflicts of Interest: The authors declare no conflicts of interest.

References

1. Lucas, L.L.; Unterweger, M.P. Comprehensive Review and Critical Evaluation of the Half-Life of Tritium. *J. Res. Natl. Inst. Stand. Technol.* **2000**, *105*, 541. [CrossRef] [PubMed]
2. Rozanski, K.; Gonfiantini, R.; Araguas-Araguas, L. Tritium in the Global Atmosphere: Distribution Patterns and Recent Trends. *J. Phys. G Nucl. Part. Phys.* **1991**, *17*, S523–S536. [CrossRef]
3. Mook, W.G. *Environmental Isotopes in the Hydrological Cycle, Principle and Applications, I–IV*; Technical document in hydrology; UNESCO: Paris, France, 2001.
4. Kaufman, S.; Libby, W.F. The Natural Distribution of Tritium. *Phys. Rev.* **1954**, *93*, 1337–1344. [CrossRef]
5. Gröning, M.; Rozanski, K. Uncertainty Assessment of Environmental Tritium Measurements in Water. *Accred. Qual. Assur.* **2003**, *8*, 359–366. [CrossRef]
6. Clark, I.D.; Fritz, P. *Environmental Isotopes in Hydrogeology*, 1st ed.; CRC Press: Boca Raton, FL, USA, 2013; ISBN 978-0-429-06957-4.
7. Juhlke, T.R.; Sültenfuß, J.; Trachte, K.; Huneau, F.; Garel, E.; Santoni, S.; Barth, J.A.C.; Van Geldern, R. Tritium as a Hydrological Tracer in Mediterranean Precipitation Events. *Atmos. Chem. Phys.* **2020**, *20*, 3555–3568. [CrossRef]
8. Hanslík, E.; Ivanovová, D.; Jedináková-Křížová, V.; Juranová, E.; Šimonek, P. Concentration of Radionuclides in Hydrosphere Affected by Temelín Nuclear Power Plant in Czech Republic. *J. Environ. Radioact.* **2009**, *100*, 558–563. [CrossRef]
9. Gusyev, M.A.; Toews, M.; Morgenstern, U.; Stewart, M.; White, P.; Daughney, C.; Hadfield, J. Calibration of a Transient Transport Model to Tritium Data in Streams and Simulation of Groundwater Ages in the Western Lake Taupo Catchment, New Zealand. *Hydrol. Earth Syst. Sci.* **2013**, *17*, 1217–1227. [CrossRef]
10. Marang, L.; Siclet, F.; Luck, M.; Maro, D.; Tenailleau, L.; Jean-Baptiste, P.; Fourré, E.; Fontugne, M. Modelling Tritium Flux from Water to Atmosphere: Application to the Loire River. *J. Environ. Radioact.* **2011**, *102*, 244–251. [CrossRef] [PubMed]
11. Schubert, M.; Siebert, C.; Knoeller, K.; Roediger, T.; Schmidt, A.; Gilfedder, B. Investigating Groundwater Discharge into a Major River under Low Flow Conditions Based on a Radon Mass Balance Supported by Tritium Data. *Water* **2020**, *12*, 2838. [CrossRef]
12. Galeriu, D.; Melintescu, A. Research and Development of Environmental Tritium Modelling. *Fusion Sci. Technol.* **2011**, *60*, 1232–1237. [CrossRef]
13. Zhao, C.; Wang, G.; Zhang, M.; Wang, G.; De With, G.; Bezhenar, R.; Maderich, V.; Xia, C.; Zhao, B.; Jung, K.T.; et al. Transport and Dispersion of Tritium from the Radioactive Water of the Fukushima Daiichi Nuclear Plant. *Mar. Pollut. Bull.* **2021**, *169*, 112515. [CrossRef] [PubMed]
14. Jefanova, O.; Mažeika, J.; Petrošius, R.; Skuratovič, Ž. The Distribution of Tritium in Aquatic Environments, Lithuania. *J. Environ. Radioact.* **2018**, *188*, 11–17. [CrossRef] [PubMed]
15. *Lietuvos Higienos Norma HN 24:2023*; Lithuanian Hygiene Standard HN 24:2023 on Drinking Water Safety and Quality Requirements. Lithuanian Ministry of Health: Vilnius, Lithuania, 2023.
16. Momoshima, N.; Okai, T.; Inoue, M.; Takashima, Y. Tritium Monitoring around a Nuclear Power Station in Normal Operation. *Int. J. Radiat. Appl. Instrum. Part A Appl. Radiat. Isot.* **1987**, *38*, 263–267. [CrossRef]
17. Jean-Baptiste, P.; Baumier, D.; Fourré, E.; Dapoigny, A.; Clavel, B. The Distribution of Tritium in the Terrestrial and Aquatic Environments of the Creys-Malville Nuclear Power Plant (2002–2005). *J. Environ. Radioact.* **2007**, *94*, 107–118. [CrossRef]
18. International Atomic Energy Agency, Division of Nuclear Power, Vienna (Austria). *Nuclear Power Reactors in the World*, September 1981 ed.; IAEA: Vienna, Austria, 1981.
19. IAEA Energy. *Electricity and Nuclear Power Estimates for the Period up to 2050*, 1st ed.; 2024 Edition; Reference Data Series No Series; International Atomic Energy Agency: Vienna, Austria, 2024; ISBN 9789201234247.
20. Gosatomnadzor, Ministry of Emergency Situations of Belarus. Belarusian AES. Available online: https://svisloch.gov.by/uploads/files/Rochs/Belorusskaja-AES.pdf (accessed on 5 March 2025).
21. Adamovich, B.; Mikheeva, T.; Sorokovikova, E.; Belykh, O.; Paškauskas, R.; Kuzmin, A.; Fedorova, G.; Zhukava, H.; Karosienė, J. Phytoplankton of the transboundary River Viliya (Neris): Community structure and toxic cyanobacterial blooms. *Baltica* **2021**, *34*, 174–184. [CrossRef]
22. Passo, C.J.; Cook, G.T. *Handbook of Environmental Liquid Scintillation Spectrometry: A Compilation of Theory and Methods*; Packard Instrument Company: Downers Grove, IL, USA, 1994.
23. Rozanski, K.; Gröning, M. Tritium assay in water samples using electrolytic enrichment and liquid scintillation spectrometry. In *Quantifying Uncertainty in Nuclear Analytical Measurements*; IAEA-TECDOC-1401; IAEA: Vienna, Austria, 2004; pp. 195–217.
24. *ISO 9698:2010*; Water Quality—Determination of Tritium Activity Concentration—Liquid Scintillation Counting Method. International Organization for Standardization: Geneva, Switzerland, 2010.
25. Morgenstern, U.; Taylor, C.B. Ultra Low-Level Tritium Measurement Using Electrolytic Enrichment and LSC. *Isot. Environ. Health Stud.* **2009**, *45*, 96–117. [CrossRef]

26. Copia, L.; Wassenaar, L.I.; Terzer-Wassmuth, S.; Hillegonds, D.J.; Klaus, P.M.; Araguás-Araguás, L.J. Proficiency Testing of 78 International Laboratories Measuring Tritium in Environmental Waters by Decay Counting and Mass Spectrometry for Age Dating and Water Resources Assessment. *Rapid Comm Mass Spectrom.* **2020**, *34*, e8832. [CrossRef]
27. Lithuanian Hydrometeorological Service. *Hidrologijos Metraštis*; Lithuanian Hydrometeorological Service: Vilnius, Lithuania, 2019; ISSN 1822-2897.
28. Lithuanian Hydrometeorological Service. *Hidrologijos Metraštis*; Lithuanian Hydrometeorological Service: Vilnius, Lithuania, 2020; ISSN 1822-2897.
29. Lithuanian Hydrometeorological Service. *Hidrologijos Metraštis*; Lithuanian Hydrometeorological Service: Vilnius, Lithuania, 2021; ISSN 1822-2897.
30. Lithuanian Hydrometeorological Service. *Hidrologijos Metraštis*; Lithuanian Hydrometeorological Service: Vilnius, Lithuania, 2022; ISSN 1822-2897.
31. Lithuanian Hydrometeorological Service. *Hidrologijos Metraštis*; Lithuanian Hydrometeorological Service: Vilnius, Lithuania, 2023; ISSN 1822-2897.
32. Lithuanian Hydrometeorological Service. *Hidrologijos Metraštis*; Lithuanian Hydrometeorological Service: Vilnius, Lithuania, 2024; ISSN 1822-2897.
33. Baltakis, V.; Beconis, M.; Česnulevičius, A.; Dicevičienė, L.; Dvareckas, V.; Juozapavičius, G.; Jurgaitis, A.; Masiliūnas, L.; Mardosienė, D.; Mikalauskas, A.; et al. Geodynamic Processes of the Neris Valley. *Geogr. Metraštis* **1982**, *20*, 5–64.
34. Modelica Association. *Modelica®—A Unified Object-Oriented Language for Systems Modeling, Version 2023*; Modelica Association: Linköping, Sweden, 2023; Available online: https://www.modelica.org (accessed on 5 March 2025).
35. Powersim Software. *Powersim Studio User's Guide*; Powersim Software: Bergen, Norway, 2003.
36. Borshchev, A.; Grigoryev, I. *The Big Book of Simulation Modeling*; Multimethod Modeling with AnyLogic 8; The AnyLogic Company: Oakbrook Terrace, IL, USA, 2020.
37. Cao, X.; Temple, T.; Li, X.; Coulon, F.; Sui, H. Influence of particle size and organic carbon content on distribution and fate of aliphatic and aromatic hydrocarbon fractions in chalks. *Environ. Technol. Innov.* **2015**, *4*, 227–239. [CrossRef]
38. Edifor, E.E.; Brown, R.; Smith, P.; Kossik, R. Non-Adherence Tree Analysis (NATA)—An Adherence Improvement Framework: A COVID-19 Case Study. *PLoS ONE* **2021**, *16*, e0247109. [CrossRef]
39. Carter, A.; Kelly, M.; Bailey, L. Radioactive high level waste insight modelling for geological disposal facilities. *Phys. Chem. Earth Parts A/B/C* **2013**, *64*, 1–11. [CrossRef]
40. Esh, D.W.; Bradford, A.H.; Banovac, K.L.; Davis, B.J. Risks and Uncertainties Associated With High-Level Waste Tank Closure. *MRS Online Proc. Libr.* **2002**, *757*, 112. [CrossRef]
41. Pensado, O.; Mohanty, S.; Kanno, T.; Tochigi, Y. *Use of Simplified Models in the Performance Assessment of a High-Level Waste Repository System in Japan*; Academia: Prague, Czechoslovakia, 2005.
42. Vopálka, D.; Lukin, D.; Vokál, A. Modelling of Processes Occurring in Deep Geological Repository—Development of New Modules in the GoldSim Environment. *Czech. J. Phys.* **2006**, *56*, D623–D628. [CrossRef]
43. Markley, C.; Pensado, O.; Gwo, J.P.; Winterle, J.; Ahn, T.; Benke, R.; Cao, T.; González, H.; Gray, A.; He, X.; et al. *SOAR: A Model for Scoping of Options and Analyzing Risk, Version 1.0*; User Guide. ML112440119; Center for Nuclear Waste Regulatory Analyses: San Antonio, TX, USA, 2011.
44. Havlová, V.; Večerník, P.; Najser, J.; Sosna, K.; Breiter, K. Radionuclide Diffusion into Undisturbed and Altered Crystalline. *Rocks. Mineral. Mag.* **2012**, *76*, 3191–3201. [CrossRef]
45. Panik, M.; Necas, V. GOLDSIM models of long-term radiation impact of conditionally cleared radioactive material. *Prog. Nucl. Energy* **2013**, *67*, 88–97. [CrossRef]
46. Felipe-Sotelo, M.; Hinchliff, J.; Drury, D.; Evans, N.D.M.; Williams, S.; Read, D. Radial Diffusion of Radiocaesium and Radioiodide through Cementitious Backfill. *Phys. Chem. Earth Parts A/B/C* **2014**, *70–71*, 60–70. [CrossRef]
47. Jolin, W.C.; Kaminski, M. Sorbent Materials for Rapid Remediation of Wash Water during Radiological Event Relief. *Chemosphere* **2016**, *162*, 165–171. [CrossRef] [PubMed]
48. Brown, K.G.; Smith, F.; Flach, G. Goldsim dynamic-link library (dll) interface for cementitious barriers partnership (cbp) code integration–11444. In Proceedings of the 37th Annual Radioactive Waste Management Symposium 2011 Conference, Phoenix, AZ, USA, 27 February–3 March 2011.
49. Landa, J.; Hokr, M. Contaminant Transport from a Deep Geological Repository: Lumped Parameters Derived from a 3D Hydrogeological Model. *Energies* **2022**, *15*, 6602. [CrossRef]
50. Lillington, J.N.P.; Goût, T.L.; Harrison, M.T.; Iwalewa, T.M.; Farnan, I. Assessing the Effect of Radioactive Waste Glass Dissolution on Early-Stage Radionuclide Migration Using Simplified Geological Repository Monte Carlo Transport Models. *MRS Adv.* **2021**, *6*, 73–79. [CrossRef]
51. Lee, Y.M.; Hwang, Y. A comparative study between GoldSim and AMBER based biosphere assessment models for an HLW repository. In Proceedings of the Korean Nuclear Society Autumn Meeting, Changwon, Republic of Korea, 23–25 October 2024.

52. Hiergesell, R.A.; Taylor, G.A. Code-to-Code Benchmarking of the PORFLOW and GoldSim Contaminant Transport Models Using a Simple 1-D Domain-11191. Savannah River Site (SRS). In Proceedings of the WM2011 Conference, Aiken, SC, USA, 27 February–3 March 2011.
53. Cunge, J.A. On The Subject of a Flood Propagation Computation Method (Musklngum Method). *J. Hydraul. Res.* **1969**, *7*, 205–230. [CrossRef]
54. Hydrological Engineering Center. *HEC-1 Flood Hydrograph Package: User's Manual*; U.S. Army Corps of Engineers: Davis, CA, USA, 1998.
55. Nature Reseach Center Vilnius. *Neris River Tritium Model*; Zenodo: Geneva, Switzerland, 2025. [CrossRef]
56. International Atomic Energy Agency. WISER: Water Isotope System for Data Analysis, Visualization and Electronic Retrieval. Available online: https://nucleus.iaea.org/wiser (accessed on 10 May 2025).
57. Nash, J.E.; Sutcliffe, J.V. River Flow Forecasting through Conceptual Models Part I—A Discussion of Principles. *J. Hydrol.* **1970**, *10*, 282–290. [CrossRef]
58. РУП «Белорусская Атомная Электростанция»—Главная. Available online: https://www.belaes.by/ru/ (accessed on 9 July 2025).
59. World Health Organization. *Guidelines for Drinking-Water Quality*; WHO: Geneva, Switzerland, 2011.
60. EUROPA—RADD—Home. Available online: https://europa.eu/radd/ (accessed on 4 June 2025).
61. Moriasi, D.N.; Arnold, J.G.; Van Liew, M.W.; Bingner, R.L.; Harmel, R.D.; Veith, T.L. Model Evaluation Guidelines for Systematic Quantification of Accuracy in Watershed Simulations. *Trans. ASABE* **2007**, *50*, 885–900. [CrossRef]
62. Ritter, A.; Muñoz-Carpena, R. Performance Evaluation of Hydrological Models: Statistical Significance for Reducing Subjectivity in Goodness-of-Fit Assessments. *J. Hydrol.* **2013**, *480*, 33–45. [CrossRef]
63. Moriasi, D.N.; Gitau, M.W.; Pai, N.; Daggupati, P. Hydrologic and water quality models: Performance measures and evaluation criteria. *Trans. ASABE* **2015**, *58*, 1763–1785. [CrossRef]
64. Fernandes, A.P.; Fonseca, A.R.; Pacheco, F.A.; Fernandes, L.S. Water quality predictions through linear regression-A brute force algorithm approach. *MethodsX* **2023**, *10*, 102153. [CrossRef]
65. Jung, W.S.; Kim, S.E.; Kim, Y.D. Prediction of Surface Water Quality by Artificial Neural Network Model Using Probabilistic Weather Forecasting. *Water* **2021**, *13*, 2392. [CrossRef]
66. Jean-Baptiste, P.; Fontugne, M.; Fourré, E.; Marang, L.; Antonelli, C.; Charmasson, S.; Siclet, F. Tritium and Radiocarbon Levels in the Rhône River Delta and along the French Mediterranean Coastline. *J. Environ. Radioact.* **2018**, *187*, 53–64. [CrossRef] [PubMed]
67. Eyrolle, F.; Lepage, H.; Antonelli, C.; Morereau, A.; Cossonnet, C.; Boyer, P.; Gurriaran, R. Radionuclides in Waters and Suspended Sediments in the Rhone River (France)—Current Contents, Anthropic Pressures and Trajectories. *Sci. Total Environ.* **2020**, *723*, 137873. [CrossRef]
68. Bodereau, N.; Eyrolle, F.; Copard, Y.; Dumoulin, J.-P.; Lepage, H.; Giner, F.; Mourier, D.; Gurriaran, R. Carbon-14 Cycling in a Nuclearized River: A First Study in the Downstream Part of the Rhône River (France). *Sci. Total Environ.* **2024**, *954*, 176502. [CrossRef]
69. Siclet, F.; Luck, M.; Le Dortz, J.G.; Damois, C.; Ciffroy, P.; Hendrickx, F.; Courivaud, J.R. Radionuclides Concentrations in the Loire River System Resulting from Routine Discharges of Five Nuclear Power Plants: Assessment of Dose to Man. *Radioprotection* **2002**, *37*, 399–410. [CrossRef]
70. Goutal, N.; Luck, M.; Boyer, P.; Monte, L.; Siclet, F.; Angeli, G. Assessment, Validation and Intercomparison of Operational Models for Predicting Tritium Migration from Routine Discharges of Nuclear Power Plants: The Case of Loire River. *J. Environ. Radioact.* **2008**, *99*, 367–382. [CrossRef]
71. Sizonenko, V.; Sinitsyn, I. Application of a Modified Aggregated Dead Zone Model to Estimate Radionuclide Transport in Running Surface Water Bodies. *Ecol. Model.* **2025**, *507*, 111187. [CrossRef]
72. Pujol, L.; Sanchez-Cabeza, J.A. Natural and Artificial Radioactivity in Surface Waters of the Ebro River Basin (Northeast Spain). *J. Environ. Radioact.* **2000**, *51*, 181–210. [CrossRef]
73. Baeza, A.; Brogueira, A.M.; Carreiro, M.C.V.; García, E.; Gil, J.M.; Miró, C.; Sequeira, M.M.; Teixeira, M.M.R. Spatial and Temporal Evolution of the Levels of Tritium in the Tagus River in Its Passage through Caceres (Spain) and the Alentejo (Portugal). *Water Res.* **2001**, *35*, 705–714. [CrossRef]
74. Baeza, A.; García, E.; Miró, C.; Periáñez, R. Modelling the Spatio-Temporal Evolution of 3H in the Waters of the River Tagus. *J. Environ. Radioact.* **2006**, *86*, 367–383. [CrossRef]
75. Grahek, Ž.; Breznik, B.; Stojković, I.; Coha, I.; Nikolov, J.; Todorović, N. Measurement of Tritium in the Sava and Danube Rivers. *J. Environ. Radioact.* **2016**, *162–163*, 56–67. [CrossRef] [PubMed]
76. Hanslík, E.; Ivanovová, D.; Juranová, E.; Šimonek, P.; Jedináková-Křížová, V. Monitoring and Assessment of Radionuclide Discharges from Temelín Nuclear Power Plant into the Vltava River (Czech Republic). *J. Environ. Radioact.* **2009**, *100*, 131–138. [CrossRef] [PubMed]

77. Hanslík, E.; Marešová, D.; Juranová, E.; Sedlářová, B. Comparison of Balance of Tritium Activity in Waste Water from Nuclear Power Plants and at Selected Monitoring Sites in the Vltava River, Elbe River and Jihlava (Dyje) River Catchments in the Czech Republic. *J. Environ. Manag.* **2017**, *203*, 1137–1142. [CrossRef] [PubMed]
78. Simek, P.; Kořínková, T.; Svetlik, I.; Povinec, P.P.; Fejgl, M.; Malátová, I.; Tomaskova, L.; Stepan, V. The Valley System of the Jihlava River and Mohelno Reservoir with Enhanced Tritium Activities. *J. Environ. Radioact.* **2017**, *166*, 83–90. [CrossRef]
79. Hanslík, E.; Marešová, D.; Juranová, E.; Sedlářová, B. Kinetics of 3 H, 90 Sr and 137 Cs Content Changes in Hydrosphere in the Vltava River System (Czech Republic). *J. Environ. Radioact.* **2018**, *188*, 1–10. [CrossRef]
80. Panov, A.; Trapeznikov, A.; Trapeznikova, V.; Korzhavin, A. Influence of Operation of Thermal and Fast Reactors of the Beloyarsk NPP on the Radioecological Situation in River Ecosystems. *J. Environ. Radioact.* **2023**, *264*, 107209. [CrossRef] [PubMed]
81. Chapra, S.C. *Surface Water-Quality Modeling*; Waveland Press: Long Grove, IL, USA, 2008.
82. Punys, P.; Adamonyte, I.; Kvaraciejus, A.; Martinaitis, E.; Vyciene, G.; Kasiulis, E. Riverine Hydrokinetic Resource Assessment. A Case Study of a Lowland River in Lithuania. *Renew. Sustain. Energy Rev.* **2015**, *50*, 643–652. [CrossRef]
83. Fischer, H.B.; List, E.J.; Koh, R.C.Y.; Imberger, J.; Brooks, N.H. *Mixing in Inland and Coastal Waters*; Academic Press: New York, NY, USA, 1979; pp. 104–138.
84. Punys, P.; Adamonytė, I.; Kvaraciejus, A. Hydraulic Geometry of the River Neris for the Assessment of Hydrokinetic Resources. *Rural. Dev.* **2013**, *6*, 418–423. [CrossRef]
85. Leopold, L.B.; Maddock, T. *The Hydraulic Geometry of Stream Channels and Some Physiographic Implications*; U.S. Geological Survey Professional Paper 252; US Government Printing Office: Washington, DC, USA, 1953.